Magnetic behaviour of the compound $CeNi_2Al_5$: double-k magnetic structure

1995 J. Phys.: Condens. Matter 7 8337

(http://iopscience.iop.org/0953-8984/7/43/012)

J. Phys.: Condens. Matter 7 (1995) 8337–8350. Printed in the UK

Magnetic behaviour of the compound $CeNi_2Al_5$: double-k magnetic structure

J X Boucherle†*, P Burlet†*, F Givord†*, Y Isikawa‡, R Neudert§, D Schmitt¶ and H Schober§

† CEA, Département de Recherche Fondamentale sur la Matière Condensée, SPSMS/MDN, CENG, 17 rue des Martyrs, 38054 Grenoble Cedex 9, France
‡ Department of Physics, Toyama University, Toyama 930, Japan
§ ILL, BP 156, 38042 Grenoble Cedex 9, France
¶ Laboratoire L Néel, CNRS, BP 166, 38042 Grenoble Cedex 9, France

Received 30 May 1995

Abstract. The orthorhombic Kondo compound $CeNi_2Al_5$ is magnetically ordered below 2.6 K. Earlier neutron diffraction experiments have led to a sine-wave modulated magnetic structure, with a single three-component propagation vector $k = (0.500, 0.405, 0.083)$ and a moment in the (a, b) plane, 8° tilted from the b direction towards the a one. The crystal electric field coefficients, previously deduced from the thermal variation of the susceptibilities along the three principal axes, have been confirmed by neutron spectroscopy. They lead to an easy magnetization direction along b, in agreement with the magnetization curves. The discrepancy between earlier neutron and magnetization results concerning the orientation of the moment was solved by performing a new neutron diffraction experiment under uniaxial stress (an applied magnetic field). In fact, the magnetic structure is a double-k structure with $k = (0.500, 0.405, 0.083)$ and $k' = (-0.500, 0.405, 0.083)$. The resulting moment can then be aligned along the easy magnetization direction b. A deeper insight into the magnetic properties of $CeNi_2Al_5$ suggests that the magnetic transition at 2.6 K could be of first order. Additional interactions other than isotropic exchange interactions and crystal electric field effects are probably present in this compound.

1. Introduction

Many ternary intermetallic compounds containing cerium atoms have recently been investigated and various types of dense-Kondo or valence-fluctuating compounds have been found. In the Ce–Ni–Al system, $CeNi_2Al_5$ is a dense-Kondo compound [1,2] with a magnetic transition at 2.6 K. In particular, the temperature dependence of its resistivity [1] is typical of the presence of Kondo effects: it exhibits a minimum around 30 K, followed by a $\ln T$ behaviour as temperature decreases.

Moreover, the crystal structure of $CeNi_2Al_5$ is body-centred orthorhombic [3,4], leading to strong crystal electric field (CEF) effects on the Ce atoms which are all located on one single crystallographic site. Magnetization measurements, performed on a single crystal along the three principal symmetry directions [5], show a very large anisotropy with b as the easy magnetization axis (figure 1). The anisotropy of the susceptibilities and the presence of bumps in their thermal variations (insets in figure 3) were used to determine

* CNRS staff.

0953-8984/95/438337+14$19.50

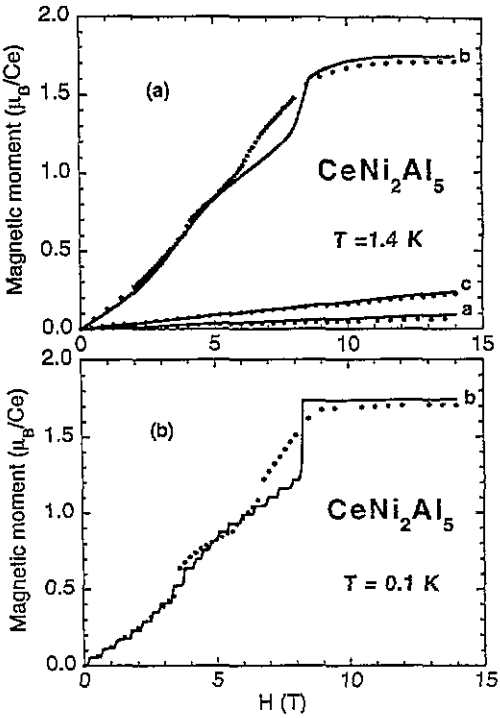

Figure 1. Magnetization of a $CeNi_2Al_5$ single crystal (*a*) at $T = 1.4$ K along the three main axes, (*b*) at $T = 0.1$ K along the easy axis *b*. The points are *experimental values and the full curves are calculated* using the CEF parameters from table 1, row (*b*).

the CEF parameters. However, such a determination, from only one type of measurement, can lead to several solutions [5].

Neutron diffraction experiments were performed at 1.5 K to study the $CeNi_2Al_5$ magnetic structure [5, 6]. Experiments on powder led to a sine-wave modulated structure with a complex three-component propagation vector $k = (0.500, 0.405, 0.083)$. Experiments on a single crystal have shown that the moment has a maximum amplitude of 1.45 μ_B, but it is not oriented along *b* in the hypothesis of a single-*k* structure: it is tilted 8° from the *b* direction towards the *a* direction, in the (*a*, *b*) plane. This results is in contradiction with the magnetization measurement results: the *a* direction was found to be the axis of most difficult magnetization, with a huge anisotropy, the ratio between the magnetizations along *b* and *a* being of the order of 20 (figure 1). However, some low-temperature nuclear orientation experiments had already led to similar conclusions [7]: at 10 mK, the moment had been deduced to be in the (*a*, *b*) plane, at 27° from the *b* axis.

Two types of experiment were thus undertaken, in order to solve the discrepancy between the magnetization and the neutron diffraction results, concerning the direction of the magnetic moment. The CEF excitations were observed by inelastic neutron scattering in order to get information on the splitting of the $4f^1$ ground-state *J* multiplet and to check the CEF parameters. Furthermore, a new neutron diffraction experiment was performed to check the magnetic structure and, in particular, a uniaxial stress was applied on the single crystalline sample to search for the possibility of a multi-*k* structure.

2. Experimental details

The samples were the same as those used for the previous experiments [5, 6]. The powder for

the inelastic scattering and the single crystal for the structure determination were extracted from the same ingot. The isomorphous non-magnetic compound $LaNi_2Al_5$ was also prepared in order to study phonon scattering and use it to correct the spectra from their contributions.

The inelastic neutron scattering (INS) experiments were performed on the DN6 time-of-flight spectrometer at the Siloé reactor (CEN Grenoble). Two incident energies of the neutrons were used: 17.4 meV and 69.6 meV. Spectra were collected for scattering angles 2θ ranging from 23–99°, in order to follow the angular dependence of the magnetic, as well as phonon, scatterings.

Neutron diffraction on the single crystal was performed on the DN3 two-axis diffractometer at the Siloé reactor (CEN Grenoble), at 1.5 K and with an incident wavelength of 1.544Å. A magnetic field up to 5 T, produced by a superconducting coil, could be applied vertically.

3. Inelastic neutron scattering

First INS experiments on $CeNi_2Al_5$ were carried out at low temperatures (20 K) with an incident neutron energy of 69.6 meV. They revealed one strong signal of magnetic origin around 18 meV, which was interpreted as resulting from a transition between the ground and first excited state of the Ce multiplet (see the inset in figure 2). Although there were signs of magnetic intensities at higher energies, the low signal-to-noise ratio did not permit us to determine the energy of the second excited state without ambiguity.

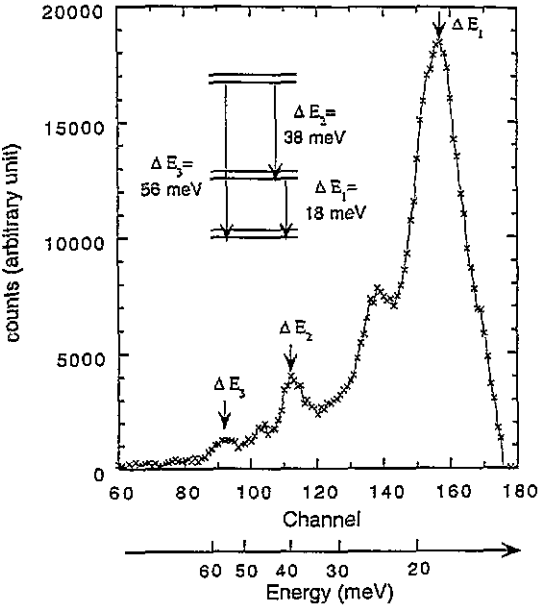

Figure 2. Difference between the INS spectra of $CeNi_2Al_5$ and $LaNi_2Al_5$ measured at 300 K and 17.4 meV (summed over all detectors).

The investigations were then continued at room temperature, with the aim of completing the level scheme by observing the transition between the first and second excited states. The first experiments at room temperature were done in up-scattering mode using 17.4 meV neutrons. Due to the relatively high flux of incident neutrons at this energy, we could achieve good statistics within the limited time available. The phonon contributions to the well

structured spectra were evaluated by performing identical experiments on the isomorphous non-magnetic reference sample $LaNi_2Al_5$. The difference between $CeNi_2Al_5$ and $LaNi_2Al_5$ spectra after proper normalization and background correction is shown in figure 2 (sums are over all scattering angles). An analysis of the k-dependence identifies three out of the four peaks as magnetic: at 18 meV (210 K), 38 meV (440 K) and 56 meV (650 K). The fourth peak, around 25 meV, originates from differences in the phonon spectra and scattering length of the magnetic and non-magnetic compounds. These three peaks already allowed us to discriminate among the two sets of CEF parameters, used in [5] to explain the magnetization results. Set 1, yielding CEF excitation energies of $\Delta_1 = 231$ K and $\Delta_2 = 638$ K, with no reduction of the moment, is in agreement with the INS data.

Although the excitation energies could be determined with sufficient precision from the up-scattering data, the extraction of the magnetic scattering intensities was impossible. Due to the differences in the phonon spectra as well as scattering lengths of magnetic and reference sample, the extraction of the magnetic scattering intensities from the time-of-flight data demands rather sophisticated correction procedures [8]. These procedures exploit the variation of inelastic scattering intensities between the high- and low-angle banks of the non-magnetic reference sample. Under the assumption that this variation, in what concerns the phononic part, is identical for both the magnetic and non-magnetic compounds, it can be used to discriminate magnetic from non-magnetic scattering. We will not go into the details of this procedure, but simply state that it cannot be applied successfully to the 17.4 meV data. The momentum transfers involved are to small to make sure that no magnetic contributions are present in the high-angle bank of the magnetic sample.

We therefore repeated the 69.6 meV low-temperature measurements at room temperature. The phonon-corrected spectra of $CeNi_2Al_5$ for scattering angles in the range 23–41° are presented in figure 3. As expected from the 17.4 meV data, two clear magnetic peaks are observed at 18 meV and 38 meV. There is some indication of a third excitation around 56 meV. However, the statistical errors, as in the low-temperature experiment, are very large. The fact that the already small intensity of this excitation is distributed over a large number of time channels implies a poor signal-to-noise ratio. Due to this poor ratio, small errors within the subtraction of the non-magnetic contributions may appreciably falsify the result.

We would like to point out that the available experimental densities of states for systems like $CeAl_2$ [9] and Ni_3Al [10] do not extend beyond 40 meV. The phonon spectrum of $CeNi_2Al_5$ seems to be harder, featuring clear non-magnetic intensities beyond this threshold. Figure 4 shows the generalized phononic density-of-states for the reference compound $LaNi_2Al_5$ as obtained under the incoherent approximation. The multiple phonon contributions to the spectra have been corrected in a self-consistent way using an effective mass of $m_{\text{eff}} = 67.3$ amu and average scattering power of $\sigma_{\text{ac}} = 6.8$ barns. The presence of excitations above 40 meV is observed and may be explained by short bond lengths (the shortest distance Ni–Al is 2.27 Å). A complete lattice dynamical study would be necessary to clarify this point.

The INS intensities can be calculated [11, 12] as a function of the CEF parameters V_l^m used in the expression of the CEF Hamiltonian $\mathcal{H}_{CEF}$. For an orthorhombic symmetry on the cerium sites, it can be expressed as

$$\mathcal{H}_{CEF} = \alpha_J(V_2^0 O_2^0 + V_2^2 O_2^2 + \beta_J(V_4^0 O_4^0 + V_4^2 O_4^2 + V_4^4 O_4^4) + \gamma_J(V_6^0 O_6^0 + V_6^2 O_6^2 + V_6^4 O_6^4 + V_6^6 O_6^6)$$

where the O_l^m are the Stevens operators and α_J, β_J and γ_J the Stevens coefficients. In the case of cerium atoms ($J = 5/2$), γ_J is zero and only the second- and fourth-order terms remain.

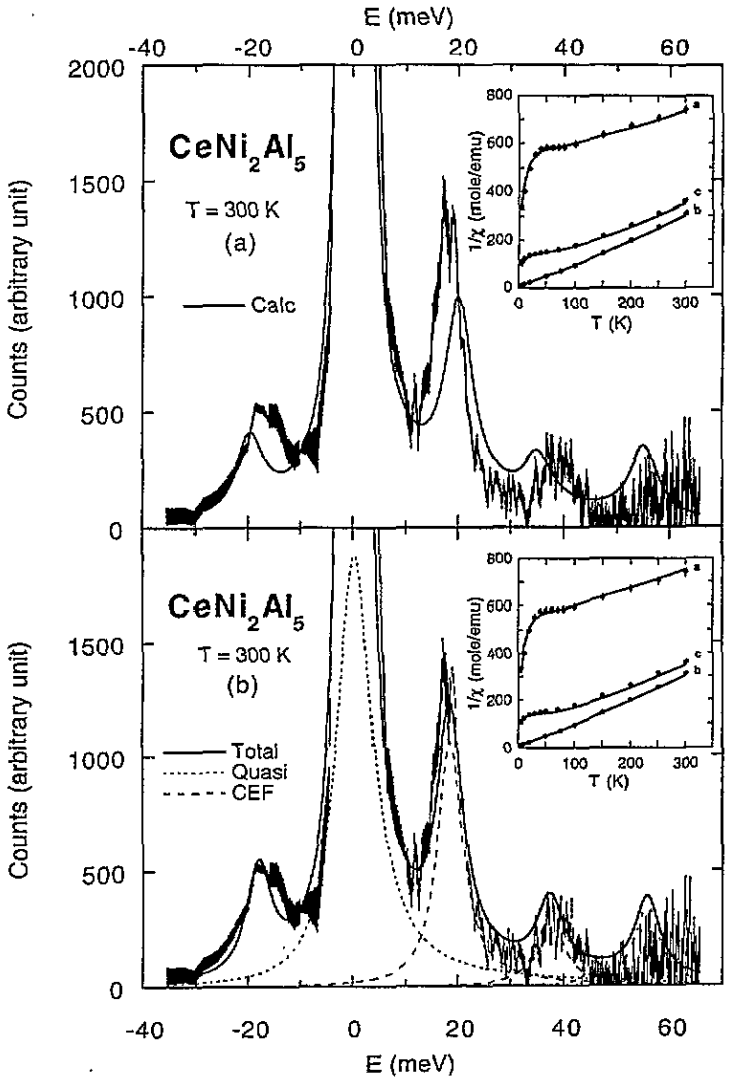

Figure 3. Magnetic spectral response obtained at 300 K for an incident neutron energy of 69.6 meV at $\theta_{moy} = 32°$. Insets show the reciprocal susceptibilities against temperature. Lines are calculated curves: (*a*) with CEF parameters from [5], (*b*) with refined CEF parameters.

For susceptibility and magnetization calculations, the total Hamiltonian is obtained by adding a Zeeman term $\mathcal{H}_z$, which includes the coupling between the 4f magnetic moment J and the magnetic fields, applied field H and exchange field H_{ex}:

$$\mathcal{H}_z = -M \cdot (H + H_{ex}) + \tfrac{1}{2}\langle M \rangle \cdot H_{ex}$$

with $M = g_J \mu_B J$.

The term $\frac{1}{2}\langle M \rangle \cdot H_{ex}$ is to ensure not double-counting the same interaction energy in the total energy of the system. In the paramagnetic region, or at sufficiently high applied magnetic fields in the ordered state, the exchange field is

$$H_{ex} = n\langle M \rangle = g_J \mu_B \langle J \rangle$$

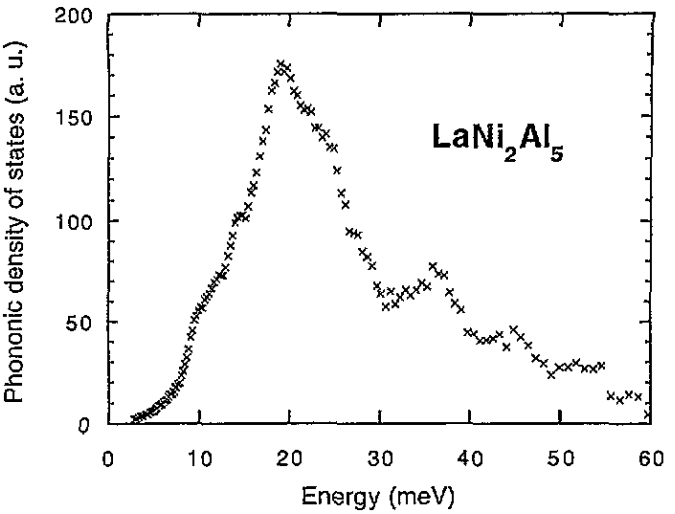

Figure 4. Generalized phononic density of states obtained from the INS spectra for $LaNi_2Al_5$.

where n is the bilinear exchange parameter.

Figure 3(*a*) shows a comparison of the experimental intensities with calculations based on set 1 of CEF and exchange parameters used in [5]. The inset shows the reciprocal susceptibilities from which these parameters were obtained. Both peak positions and intensities are rather well reproduced by the calculation. There is a clear signature of quasi-elastic magnetic scattering (half-width $\Gamma_0/2$) in the experimental data. This is to be expected for a Kondo system. We have tried to improve the agreement between experiment and theory by refining the CEF and exchange parameters simultaneously to the INS and magnetic data (susceptibility curves and magnetization along b at 1.4 K in a 14 T field). The result is shown in figure 3(*b*). While considerably improving the agreement with the INS data, we still obtain a very good fit of the reciprocal susceptibilities. The parameter values are listed in table 1 together with those of [5]. The changes are very small. The wavefunctions corresponding to the various levels are given in table 2. The combined analysis of magnetic and INS experiments has, therefore, allowed us to determine unambiguously the CEF parameters in $CeNi_2Al_5$.

Table 1. Parameters obtained from refinements of the neutron spectroscopy and magnetic results. (*a*) Fixed CEF and exchange parameters from [5]. (*b*) Refined parameters. $\Gamma/2$ and $\Gamma_0/2$ are the halfwidth of the excitation lines and of the quasi-elastic contribution, respectively.

	V_2^0 (K)	V_2^2 (K)	V_4^0 (K)	V_4^2 (K)	V_4^4 (K)	n (T/μ_B)	$\Gamma/2$	$\Gamma_0/2$	χ^2
(*a*)	278(4)	743(24)	42(4)	−622(15)	622(26)	−3.5(0.1)	3.2(0.1)	6.1(1.4)	18
(*b*)	292(7)	776(9)	52(6)	−584(20)	584(19)	−4.2(0.1)	3.0(0.1)	4.0(0.5)	6

Table 2. CEF levels in $CeNi_2Al_5$.

Energy (K)	Wavefunction
646	$-0.463\vert \pm 5/2\rangle + 0.814\vert \pm 1/2\rangle - 0.351\vert \mp 3/2\rangle$
212	$-0.276\vert \pm 5/2\rangle + 0.382\vert \pm 1/2\rangle + 0.924\vert \mp 3/2\rangle$
0	$0.886\vert \pm 5/2\rangle + 0.437\vert \pm 1/2\rangle - 0.155\vert \mp 3/2\rangle$

4. Magnetic structure

For the magnetic structure previously determined [4,5] with a propagation vector of type (k_x, k_y, k_z), four magnetic domains can exist in the crystal, corresponding to the four equivalent vectors obtained by the symmetry operations of the crystal. The diffraction pattern consists of eight magnetic peaks located at $\boldsymbol{H} \pm \boldsymbol{k}$ around each Brillouin zone centre $\boldsymbol{H}$ and the intensities of these magnetic peaks depend on the domain distribution. In fact, the eight reflections $(0\ 0\ 0)^{\pm}$ associated with the propagation vectors $(\pm k_x, \pm k_y, \pm k_z)$ were found to have the same intensity [4] and the four domains are equivalent. However, such a structure is indistinguishable from the structure resulting from a multi-$\boldsymbol{k}$ ordering with fewer magnetic domains.

One way to modify the domain distribution is to apply a magnetic field in an appropriate direction and then to cool down the crystal through T_N. The crystal was oriented inside the cryomagnet with the a direction almost vertical, i.e. with a small misorientation of about 5° towards b and 5° towards c. When the magnetic field is applied vertically, its orientation with regards to the four moments in the four domains is different. In the presence of the field, the intensities of the eight magnetic peaks will show four different behaviours unless the structure is not mono-$\boldsymbol{k}$. If the structure is double-$\boldsymbol{k}$, two different behaviours only should be observed, corresponding to two magnetic domains.

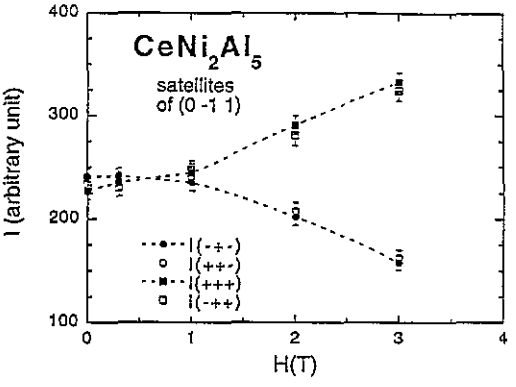

Figure 5. Variation with the field of the intensities of four equivalent satellites. Each point is obtained after cooling from the paramagnetic region under the considered field. $I(-\ +\ -)$ corresponds to the reflection $(0, -1, 1) + (-k_x, +k_x, -k_z)$.

Various magnetic fields ranging from 0–3 T were applied in the paramagnetic state, and for each field the temperature was then decreased below T_N. The intensities of the eight satellites of the $(0\ -1\ 1)$ reflection were measured at 1.5 K. Their variations are shown in figure 5. The intensities of the $+\boldsymbol{k}$ and $-\boldsymbol{k}$ reflections vary in the same way and only the $+\boldsymbol{k}$ ones are represented. One can notice that the satellites associated with the propagation vectors $(+k_x, +k_y, +k_z)$ and $(-k_x, +k_y, +k_z)$ increase in exactly the same way, whereas the satellites associated with the propagation vectors $(+k_x, +k_y, -k_z)$ and $(-k_x, +k_y, -k_z)$ also decrease in the same way. There are then only two magnetic domains and the magnetic structure is a double-$\boldsymbol{k}$ structure with propagation vectors $\boldsymbol{k} = (0.500, 0.405, 0.083)$ and $\boldsymbol{k}' = (-0.500, 0.405, 0.083)$. The magnetic satellites $(h, k, l) \pm \boldsymbol{k}$, that had been indexed with the propagation vector $\boldsymbol{k}$ and that were satisfying the reflection condition $h+k+l = 2n$ for a body-centred structure, can also be indexed as $(h \pm 1, k, l) \pm \boldsymbol{k}'$, because $\boldsymbol{k} - \boldsymbol{k}' = (1\ 0\ 0)$. This new indexation does not satisfy the above reflection condition. The magnetic structure can then not be body-centred, the two atoms at the origin and at the centre of the cell belonging no more to the same Bravais lattice.

The expression of the resulting moment is given by the Fourier expansion

$$m(r) = \sum_{k_i} m_{k_i} \exp(2i\pi k_i \cdot r).$$

As no third-order satellite has been observed at 1.5 K [5], the moment $m(r)$ for a mono-k structure, is the summation on the Fourier components $m_{\pm k}$ and varies sinusoidally:

$$m(r) = 2|m_k| \cos(2\pi k_i \cdot r - \phi)$$

where ϕ is a phase characteristic of the atomic site and is generally taken to be 0 if there is only one site. The maximum amplitude of the moment is $m_{max} = 2|m_k| = 1.45\mu_B$.

For a double-k structure, the moment $M(r)$ is the summation on the Fourier components $M_{\pm k}$ and $M_{\pm k'}$. We then get

$$M(r) = 2|M_k| \cos(2\pi k \cdot r - \phi - \Phi) + 2|M_{k'}| \cos(2\pi k' \cdot r - \phi - \Phi')$$

where Φ and Φ' are the phases corresponding to $M_{\pm k}$ and $M_{\pm k'}$.

If the Fourier component associated with $k = (k_x, k_y, k_z)$ is $M_k = (M_{kx}, M_{ky}, M_{kz})$, the Fourier component associated with $k' = (-k_x, k_y, k_z)$ will be, by symmetry considerations, $M_{k'} = (-M_{kx}, M_{ky}, M_{kz})$. As previously found [4], $M_{kz} = 0$. $M_{\pm k}$ and $M_{\pm k'}$ are symmetric relative to the b direction with the angle $\alpha = 8°$ (figure 6).

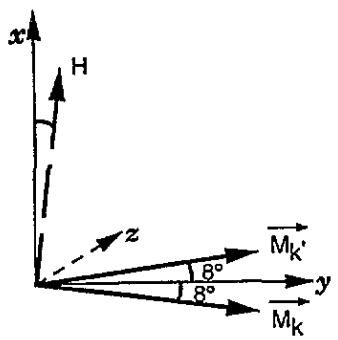

Figure 6. Fourier components $M_{\pm k}$ and $M_{\pm k'}$ associated with the two propagation vectors k and k'.

The components of the moment $M_x(r)$ and $M_y(r)$ are then

$$M_x(r) = 2M_{kx}[\cos(2\pi k \cdot r - \phi - \Phi) - \cos(2\pi k' \cdot r - \phi - \Phi')]$$

$$M_y(r) = 2M_{ky}[\cos(2\pi k \cdot r - \phi - \Phi) + \cos(2\pi k' \cdot r - \phi - \Phi')].$$

The condition necessary to get a magnetic moment aligned along the easy magnetization direction b is $M_x(r) = 0$, which involves $\cos(2\pi k \cdot r - \phi - \Phi) = \cos(2\pi k' \cdot r - \phi - \Phi')$. Taking into account the fact that $k - k' = (1\ 0\ 0)$, this condition leads to $\Phi' - \Phi = \Delta\Phi = 2\pi r_x(\pm 2n\pi)$, i.e. $\Delta\Phi = 0$ for integer values of r_x and $\Delta\Phi = \pi$ for half-integer values of r_x. The phase difference between the Fourier components of the two propagation vectors is different for the atoms at the corners and at the centre of the cell, atoms which, in fact, no longer belong to the same Bravais lattice.

The resulting magnetic moment can then be written as

$$M(r) = M_y(r) = 4M_{ky} \cos(2\pi k \cdot r - \phi - \Phi).$$

It varies sinusoidally, with a maximum amplitude $M_{max} = 4M_{ky} = 4|M_k|\cos\alpha$. Comparing the energies of the mono-k and double-k cases leads to

$$H = -Jm_k m_{-k} = -J|m_k|^2$$

$$H = -J(M_k + M_{k'})(M_{-k} + M_{-k'}) = -4J|M_k|^2\cos^2\alpha$$

that is, to $|M_k| = |m_k|/2\cos\alpha$. The maximum moment is then $M_{max} = 2|m_k| = m_{max} = 1.45\mu_B$. The value of Φ can be chosen to be zero for the propagation vector k, and the moment variation for this double-k structure is then exactly the same as for a mono-k structure: $M(r) = m(r) = 1.45\cos(2\pi k \cdot r - \phi)$. The only differences are that $M(r)$ is now aligned along b. As the atoms at the corners and at the centre of the cell do not belong to the same Bravais lattice, the phase ϕ is not necessarily the same for the two types of atoms.

5. Discussion

These two experiments, inelastic neutron scattering and magnetic structure determination under an applied stress, have allowed us to solve the discrepancy concerning the moment direction: the magnetic structure is in fact defined by two propagation vectors, the combination of which leads to a moment aligned along the b direction. This moment direction is in agreement with that given by the CEF effects, and the CEF parameters correspond to those of set 1 in [5]. The combination of two different types of experiment has led to a more precise determination of these parameters, and they are coherent with experimental results on magnetization and specific heat measurements.

5.1. Magnetization

The CEF parameter values are very close to those used in a previous paper [13] to calculate the magnetizations along the three axes in the case of modulated magnetic structures. This calculation was performed within a periodic mean-field model, which takes into account the modulation of the exchange field due to the modulation of the moment and the CEF effects [14]. As the moment variation is the same as in the case of the mono-k structure, the magnetization calculations of [13] are still valid. The magnetization of the cerium ions is calculated in a self-consistent manner using an N-site Hamiltonian:

$$\mathcal{H} = \sum_{i=1}^{N} \mathcal{H}_{CEF}(i) + \sum_{i=1}^{N} \mathcal{H}_Z(i)$$

where N is the number of magnetic ions over the considered period.

The exchange field is periodic, with the same periodicity as the magnetic moment and the successive Fourier harmonics of the exchange field H_{nk} and of the magnetic moment M_{nk} are related to each other by the expression $H_{nk} = (g_J\mu_B)^{-2}J(nk)M_{nk}$ for the different harmonics of k ($n = 0, 1, 2\ldots$).

The coupling parameters $J(nk)$ are the Fourier transforms of the exchange interactions $J(i, j)$. They can also be expressed as

$$\Theta^*(nk) = \frac{J(J+1)}{3k_B}J(nk)$$

with $J = 5/2$ for cerium, $J(0)$ and $J(k)$ are respectively connected with the paramagnetic exchange coefficient λ and with CEF susceptibility χ_0 at T_N through the relations

$$J(0) = (g_J \mu_B)^2 \lambda \qquad J(k) = (g_J \mu_B)^2 / \chi_0(T_N).$$

They lead to the values $J(0) = -2\,\mathrm{K}$ ($\Theta^*(0) = -6\,\mathrm{K}$) and $J(k) = +0.67\,\mathrm{K}$ ($\Theta^*(k) = +2\,\mathrm{K}$).

For our calculation, the case where the two atomic sites have the same phase ϕ was considered. The propagation vector was approximated by the commensurate vector $k = (1/2, 2/5, 1/12)$, which corresponds to a number of sites $N = 120$. In fact, $N = 60$ was used, this value being large enough; taking $N = 120$ or $N = 60$ does not much affect the results.

The magnetization curves at 1.4 K and 0.1 K, recalculated with the same $J(nk)$ values than in [13] (i.e. the rough values of $\Theta^*(nk = -6, 3, 2$ and 3 K for $n = 0, 1, 2$ and 3), but with the CEF parameters of table 1, are shown in figure 1. They look very similar to those of [13], and account very well for the experimental values. In particular, the anisotropy between the three principal symmetry axes is very accurately calculated. The mean slopes of the magnetization curves along the b axis are well described, as well as the critical field to reach the ferromagnetic structure ($\sim 8.5\,\mathrm{T}$). The transition observed at 3.6 T is found and corresponds to the flipping of several moments at once. Only the shape of the last transition between 7 T and 9 T is different: the observed shape is incompatible with an antiphase structure, and is probably due to Kondo effects which are not taken into account in the calculation. The presence of Kondo effects, which involve a lowering of the ordering temperature, is also confirmed by the fact that the value of $\Theta^*(k)$ had to be taken equal to 3 K instead of the value of 2 K deduced from T_N. At 0.1 K, small steps corresponding to the flipping of one moment among the 60 sites are calculated, due to the approximation of a commensurate propagation vector. As they are not observed, the propagation vector k is probably strictly incommensurate, unless the structure remains of amplitude-modulated type because of strong Kondo effects.

Table 3. Specific heat coefficients for electronic (γ) and lattice (β) contributions and Debye temperature θ_D in $CeNi_2Al_5$. The coefficients γ_0 and β_0 are obtained below T_N and used for calculating the entropy below 1 K.

γ (mJ mol^{-1} K^{-2})	β (mJ mol^{-1} K^{-4})	θ_D (K)	γ_0 (mJ mol^{-1} K^{-2})	β_0 (mJ mol^{-1} K^{-4})
8	0.35	354	250	590

5.2. Specific heat

Specific heat measurements performed from 1–30 K [1] show evidence of a sharp anomaly at $T_N = 2.6\,\mathrm{K}$ (figure 7). The specific heat can be considered as the sum of three contributions: the lattice contribution βT^3 for $T << \theta_D$ (θ_D being the Debye temperature), the electronic contribution γT, and the magnetic contribution. In order to separate the magnetic contribution to the specific heat, the γ and β values can be evaluated from the linear part of the plot of C/T against T^2 above T_N (figure 8). The deduced values are gathered in table 3, as well as the Debye temperature θ_D deduced from β by the relation $\beta = (12/5)\pi^4 n R (1/\theta_D)^3$ where n is the number of atoms per formula ($n = 8$) and R is

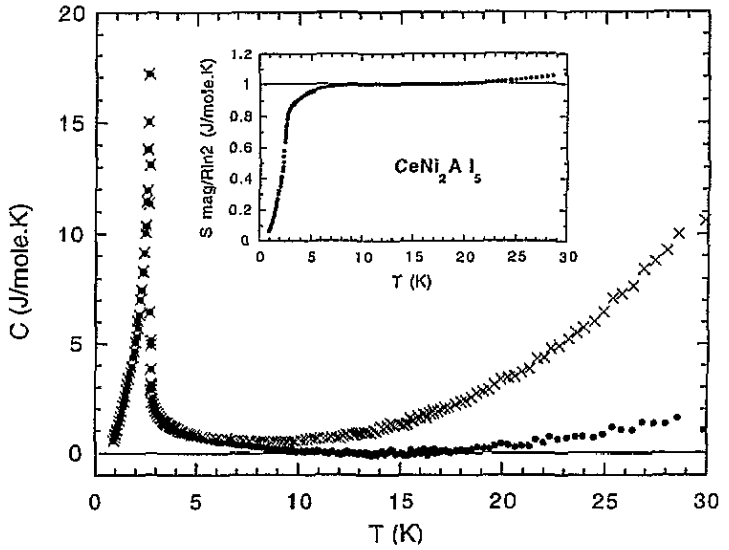

Figure 7. Temperature dependence up to 30 K of the specific heat C. Crosses are experimental values and points represent the deduced magnetic contribution. Inset: magnetic entropy S.

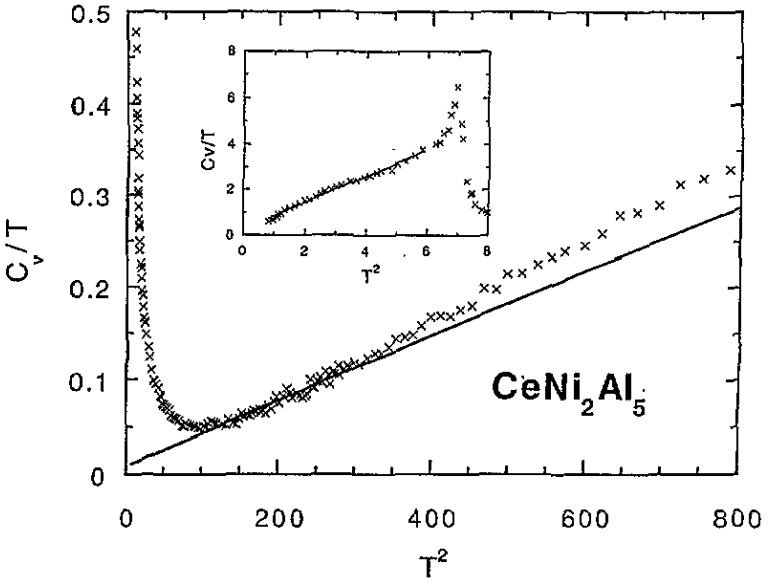

Figure 8. C/T variation against T^2. The inset shows the variation below T_N. The straight lines ($C/T = \gamma + \beta T^2$) give the γ and β coefficients.

the perfect gas constant ($R = 8.31\,\mathrm{J\,mol^{-1}\,K^{-1}}$). A rather high value of 354 K is found for θ_D, as can be expected because the Debye temperature of aluminium is itself very high (428 K). The lattice contribution to the specific heat can also be calculated from the phonon

density of states obtained from the INS measurements (see section 3). It is drawn in figure 9 and compared to the βT^3 variation in the inset. In the temperature range considered here ($T < 30$ K), the agreement between the two evaluations is excellent.

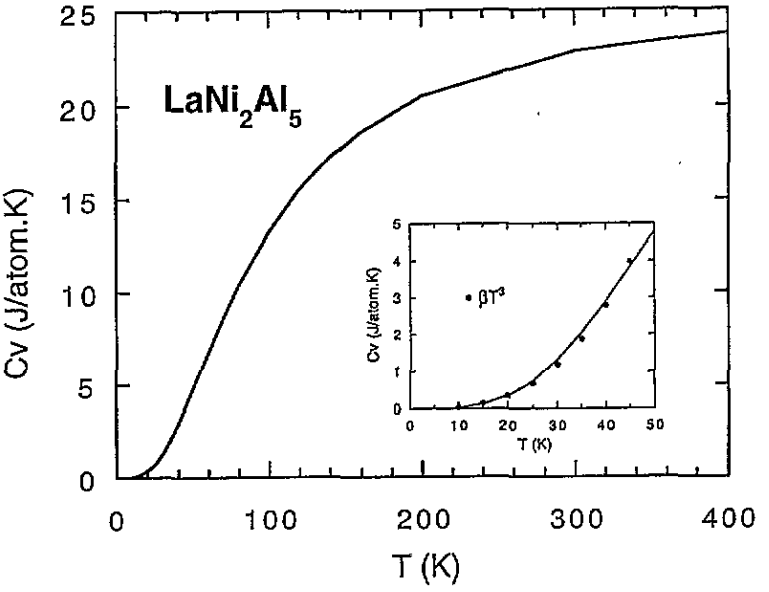

Figure 9. Lattice contribution (for one atom) to the specific heat calculated from the phononic density of states of $LaNi_2Al_5$. Inset: comparison with a βT^3 variation at low temperatures.

The magnetic specific heat is then deduced (figure 7). It vanishes around 10 K, showing the presence of short-range order above T_N. The magnetic contribution starts to increase again around 20 K. It may be due to the beginning of a spread-out Schottky anomaly centred around 100 K for the observed splitting of 209 K between the ground state and the first excited doublet.

The magnetic entropy was then calculated. The contribution of the entropy below 1 K, $S_0 = 0.38\,\mathrm{J\,mol^{-1}\,K^{-1}}$, has been estimated by extrapolation from the variation of the specific heat $C = \gamma_0 T + \beta_0 T^3$, which is observed at low temperatures, as shown in the inset of figure 8. The values of γ_0 and β_0 are given in table 3. Although these values might not be very significant because of the proximity of the Néel temperature, the value of $250\,\mathrm{mJ\,mol^{-1}\,K^{-2}}$ found for γ_0 is of the same order of magnitude as those of other Kondo compounds with close ordering temperatures: $376\,\mathrm{mJ\,mol^{-1}\,K^{-2}}$ for Ce_2Sn_5 ($T_N = 2.9$ K) [11], $180\,\mathrm{mJ\,mol^{-1}\,K^{-2}}$ for $CeCu_2$ ($T_N = 3.4$ K) [15], or 120–$155\,\mathrm{mJ\,mol^{-1}\,K^{-2}}$ for $CeAl_2$ ($T_N = 3.8$ K) [16]. The resulting entropy is drawn in the inset of figure 7. It saturates around 10 K exactly at the value $R \ln 2$, as expected for one isolated doublet ground state. This feature first justifies the validity of the data treatment and more particularly confirms the choice of a solution of the set 1-type for the CEF parameters, with no reduction of the moments. In fact, in the compounds Ce_2Sn_5 and Ce_3Sn_7 [11], the entropy saturation values reflected exactly the values of the moment reduction. The increase of the entropy above 20 K is due, as mentioned above, to the influence of the first excited doublet.

The periodic mean-field model used above to calculate the magnetizations can also be used to calculate the specific heat. The internal energy is evaluated on each site and averaged over one period to get the mean internal energy per magnetic ion. Its thermal derivative at any temperature leads to the specific heat. An analytical calculation [17] shows that, in the case of a structure with amplitude modulated (AM) moments, the specific heat discontinuity at T_N is reduced by a factor 2/3 compared to an equal moment (EM) system (for instance, a ferromagnetic or helimagnetic structure). This reduction results from the fact that, in an AM system, the periodic exchange field is zero on some sites and the corresponding moments do not contribute to the internal energy. The experimental specific heat is compared in figure 10 to those calculated in $CeNi_2Al_5$ in two cases: an EM structure and a single-k AM structure with one single exchange coefficient $J(k) = 1\,K$ ($\Theta^* = 3\,K$), i.e. a sinusoidally modulated structure. As expected for an isolated doublet, the calculated jumps at T_N are respectively $12.4\,J\,mol^{-1}\,K^{-1}$ and $8.3\,J\,mol^{-1}\,K^{-1}$, and the effect of the Kondo interactions that are present in this compound should tend to lower these values. The experimental jump is about $17\,J\,mol^{-1}\,K^{-1}$, i.e. larger than expected. The magnetic transition could then be a first-order transition, although no hysteresis effects could be observed, neither on the moment variation at T_N nor on the magnetization transitions with the applied field.

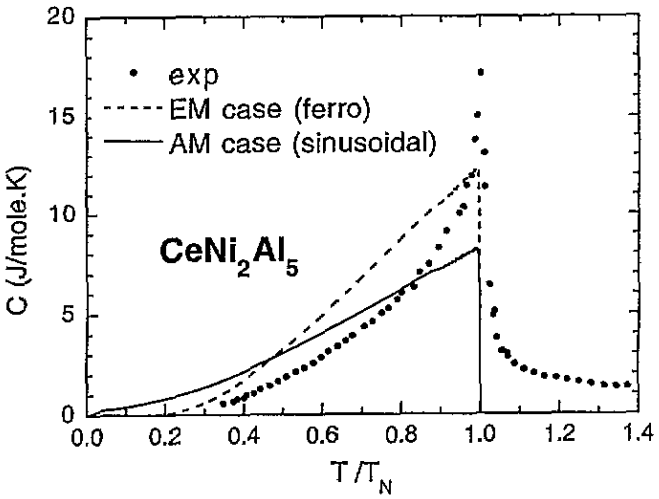

Figure 10. Experimental and calculated specific heats against T/T_N. The normalized temperature allows us to overcome the difference found in the $\Theta^*(k)$ values, because of the Kondo effects: 2 K from T_N and 3 K from the fits of the magnetization curves.

5.3. Role of additional energy terms

$CeNi_2Al_5$ presents quite peculiar properties: (i) a magnetic structure with two propagation vectors and Fourier components tilted at $\pm 8°$ from the direction of the magnetic moment, (ii) the loss of the body-centred symmetry in the magnetic state, and (iii) probably a first-order magnetic ordering transition. These unusual features are not explained within our model based on isotropic bilinear exchange interactions and crystal electric field. It can therefore be concluded that additional terms are probably important in the expression of the energy. These could originate, for example, from anisotropic exchange interactions or quadrupolar

effects. However, no lattice parameter variation could be detected at the magnetic ordering transition from the powder spectra collected on both sides of this temperature.

5.4. Conclusion

By performing two different neutron experiments, inelastic neutron scattering and the study of the evolution of the magnetic domains under an applied stress, we have been able to explain some of the discrepancies previously found in $CeNi_2Al_5$. The direction of the magnetic moment has been confirmed without ambiguity, and the crystal electric field scheme has been determined more precisely. One remaining question is the following: why is the magnetic structure not simply mono-k with the Fourier components along the easy magnetization direction b? The transition to the magnetic state is rather complex, with a loss of symmetry and a first-order transition. Some extra phenomena must be taken into account for a total understanding of this compound.

Acknowledgments

The authors wish to acknowledge A P Murani for fruitful discussions, as well as P Lejay for preparing the polycrystalline samples and M Bonnet for modifications in his refinement program.

References

[1] Isikawa Y, Mizushima T, Oyabe K, Mori K, Sato K and Kamigaki K 1991 *J. Phys. Soc. Japan* **60** 1869
[2] Isikawa Y, Mori K, Kamigaki K, Mizushima T, Oyabe K, Ueda S and Sato K 1992 *J. Magn. Magn. Mat.* **108** 157
[3] Zarechnyuk O S, Yanson T I and Rykhal R M 1983 *Izv. Akad. Nauk SSSR, Met* 4 192
[4] Parthé E and Chabot B 1984 *Handbook on the Physics and Chemistry of Rare Earths* **6** ed K A Gschneidner Jr and L Eyring (Amsterdam: North-Holland) p 113
[5] Isikawa Y, Mizushima T, Sakurai J, Mori K, Muñoz A, Givord F, Boucherle J X, Voiron J, Oliveira I S and Flouquet J 1994 *J. Phys. Soc. Japan* **63** 2349
[6] Isikawa Y, Mori K, Mizushima T, Sakurai J, Muñoz A, Givord F, Boucherle J X, Flouquet J and Oliveira I S 1994 *Physica* **194–6B** 373
[7] Nishimura K, Oliveira I S, Stone N J, Richards P, Ohya S, Isikawa Y and Mori K 1993 *Physica* **186–8B** 400
[8] Murani A P 1983 *Phys. Rev.* B **28** 2308; 1994 *Phys. Rev.* B **50** 9882
[9] Reichardt W and Nücker N 1984 *J. Phys. F: Met. Phys.* **14** L135
[10] Stassis C, Arch D, McMasters O D and Harmon B N 1981 *Phys. Rev.* B **24** 730
[11] Bonnet M, Boucherle J X, Givord F, Lapierre F, Odin J, Murani A P, Schweizer J and Stunault A 1994 *J. Magn. Magn. Mat.* **132** 289
[12] Bonnet M 1994 Private communication
[13] Boucherle J X, Givord F, Isikawa Y, Schmitt D, Tholence J L and Voiron J 1995 *J. Magn. Magn. Mat.* **140–4** 849
[14] Gignoux D and Schmitt D 1993 *Phys. Rev.* B **48** 12682
[15] Ōnuki Y, Machii Y, Shimizu Y, Komatsubara T and Fujita T 1985 *J. Phys. Soc. Japan* **54** 3562
[16] Berton A, Chaussy J, Cornut B, Lasjaunias J L, Odin J and Peyrard J 1980 *J. Magn. Magn. Mat.* **15–8** 379
[17] Blanco J A, Gignoux D and Schmitt D 1991 *Phys. Rev.* B **43** 13145; 1992 *Phys. Rev.* B **45** 2529